Superlens imaging theory for anisotropic nanostructured metamaterials with broadband all-angle negative refraction

W. T. Lu* and S. Sridhar

Department of Physics and Electronic Materials Research Institute, Northeastern University, Boston, Massachusetts 02115, USA

(Received 1 May 2008; published 2 June 2008)

We show that a metamaterial consisting of aligned metallic nanowires in a dielectric matrix has strongly anisotropic optical properties. For filling ratio $f<1/2$, the composite medium shows two surface plasmon resonances (SPRs): the transverse and longitudinal SPR with wavelengths $\lambda_t<\lambda_l$. For $\lambda>\lambda_l$, the longitudinal SPR, the material exhibits Re $\varepsilon_{\parallel}<0$, Re $\varepsilon_{\perp}>0$, relative to the nanowires axis, enabling the achievement of broadband all-angle negative refraction and superlens imaging. An imaging theory of superlens made of these media is established. High performance systems made with Au, Ag, or Al nanowires in nanoporous templates are designed and predicted to work from the infrared up to ultraviolet frequencies.

DOI: 10.1103/PhysRevB.77.233101 PACS number(s): 78.20.Ci, 42.30.Wb, 72.80.Tm, 78.66.Bz

Since the demonstration of negative refraction (NR)[1] at microwave frequencies,[2] a variety of approaches have been described to observe the phenomenon at optical frequencies.[3] There are several reasons for the interest in NR, the most prominent application being the concept of perfect lens,[4] which can lead to subwavelength imaging beyond the diffraction limit. So far, NR has been realized in periodic or quasiperiodic structures such as metamaterials[2] and photonic crystals.[5–7]

As the frequency is increased to the optical spectrum, the structure size and the unit cell size shrink to nanometer dimensions. Important developments in nanofabrication do allow the fabrication of nanostructures down to 10 nm sizes over large areas. By using either top-down nanolithography or bottom-up self assembly, it is possible to fabricate aligned nanowires in dielectric matrices with large aspect ratios. For example, in alumina nanoporous templates,[8] the pore diameter can be modified between 10 to 200 nm and the thickness can be a few nanometers up to 160 μm.[9] Typical sizes of the pore diameter of 10 nm, pore distance of 50 nm can be easily obtained. Au nanowires synthesized inside the template make a uniform array of vertical nanowires arranged parallel to each other.[10–12]

In this Brief Report, we show that such aligned nanowire structures in dielectric matrices constitute a class of indefinite index media with strongly anisotropic optical properties that can be used to achieve broadband all-angle NR (AANR) and superlens imaging. We show that these anisotropic media will have two surface plasmon resonances (SPR): a longitudinal SPR and a transverse SPR. For wavelength larger than that of the longitudinal SPR, these media are negative index metamaterials and can be used for superlens imaging[4,13] in the frequency range from the deep-infrared up to the ultraviolet. NR and superlens imaging are possible due to the anisotropic optical properties. These structures do not need to be periodic. Disordered structures can also be used for NR. Example systems are designed and demonstrated.

We consider a metal with Re $\varepsilon_m<0$ embedded in an ambient medium with positive ε_a. In the long wavelength limit, one has the Bruggeman's effective medium theory (EMT)[14–16]

$$0=f\frac{\varepsilon_m-\varepsilon_{\rm eff}}{\varepsilon_m+D\varepsilon_{\rm eff}}+(1-f)\frac{\varepsilon_a-\varepsilon_{\rm eff}}{\varepsilon_a+D\varepsilon_{\rm eff}}. \quad (1)$$

Here f is the metal filling ratio and D is a measure of the aspect ratio. The solution is

$$\varepsilon_{\rm eff}(D)=\frac{1}{2D}(\Delta\pm\sqrt{\Delta^2+4D\varepsilon_a\varepsilon_m}) \quad (2)$$

with $\Delta=f(1+D)(\varepsilon_m-\varepsilon_a)+D\varepsilon_a-\varepsilon_m$. The sign is chosen such that Im $\varepsilon_{\rm eff}>0$. For sphere inclusion, one has $D=2$.[14] For slab inclusion, $D=0$ and ∞ for the effective permittivity perpendicular and parallel to the slabs, respectively.

For cylinder inclusion with cylindrical axis in the z direction as shown in Fig. 1, one has

$$\varepsilon_x=\varepsilon_y=\varepsilon_{\rm eff}(1),$$

$$\varepsilon_z=\varepsilon_{\rm eff}(\infty)=f\varepsilon_m+(1-f)\varepsilon_a. \quad (3)$$

There exists a minimal filling ratio

$$f_{\rm min}=\varepsilon_a/(\varepsilon_a-{\rm Re}\,\varepsilon_m). \quad (4)$$

such that for $f>f_{\rm min}$, Re $\varepsilon_z<0$. Also that if $f>1/2$, Re $\varepsilon_{x,y}<0$. If one desires Re $\varepsilon_{x,y}>0$ but Re $\varepsilon_z<0$, one should have Re $\varepsilon_m<-\varepsilon_a$ so that $f_{\rm min}<1/2$. We note that for the modeling of real systems, the values of D can be different from the ones we used.[17]

The physical meaning of $f_{\rm min}$ is the following. At this filling ratio, which also corresponds to a fixed frequency or wavelength λ_l since ε_m is dispersive, the composite medium has Re $\varepsilon_z=0$, which gives strong absorption of the medium. This frequency corresponds to the so-called longitudinal

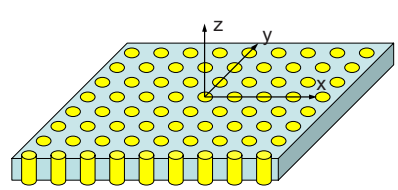

FIG. 1. (Color online) A slab of composite medium made of metal rods (yellow/light gray) embedded in a host medium (cyan/gray).

 ©2008 The American Physical Society

SPR.[18,19] For example, for a Drude metal with $\varepsilon_m = 1 - \lambda^2/\lambda_p^2$ and λ_p the plasmon wavelength, one has $\lambda_l = \lambda_p[1 + (f^{-1}-1)\varepsilon_a]^{1/2}$. Thus, λ_l is very sensitive to the filling ratio f and dielectric constant ε_a of the host medium. The increase in the filling ratio results in a blueshift of the longitudinal SPR. The smaller the refractive index of the host medium, the shorter the longitudinal SPR λ_l. High absorption is also expected for frequency at the so-called transverse SPR, which is located around the surface plasmon wavelength λ_{sp} (Re $\varepsilon_m = -\varepsilon_a$) and has very weak dependence on the filling ratio. For a Drude metal, there is a frequency range $\lambda_{t,+} < \lambda < \lambda_{t,-}$ with $\varepsilon_m(\lambda_{t,\pm}) = \varepsilon_a\{1 - 2(1-2f)^{-2} \pm 4[f(1-f)]^{1/2}(1-2f)^{-2}\}$ such that Im $\varepsilon_x > 0$, and the medium shows strong absorption. Here $\varepsilon_m(\lambda_{t,+}) > -\varepsilon_a$ and $\varepsilon_m(\lambda_{t,-}) < -\varepsilon_a$. For $f < 0.1464$, one has $\lambda_{t,-} < \lambda_l$.

For composite media with embedded Ag, Au, and Al nanowires, the effective permittivities and the absorption spectra $y = \ln[(1-R)/T]$ are calculated and shown in Fig. 2. Here R and T are the reflection and transmission intensities of waves through a slab. The optical constants are taken from Ref. 20 and fitted with polynomials. The absorption spectra clearly show the longitudinal SPRs for the P-polarized waves.

When the metamaterial has Re $\varepsilon_z < 0$ and Re $\varepsilon_{x,y} > 0$, this so-called indefinite medium[21] has unusual wave refraction phenomena and can be used for NR and superlens imaging for incident waves along the nanowire axis. We consider a slab of such medium whose surface is along the x axis and surface normal is along the z axis as shown in Fig. 3(b). We assume the relative permeability is of unity. For the P polarization with the magnetic field in the y direction and the electric field in the xz plane, the dispersion is $k_z^2 = \varepsilon_x k_0^2 - \varepsilon_x k_x^2/\varepsilon_z$. Here $k_0 = 2\pi/\lambda$ the wave number in free space. When Re $\varepsilon_z < 0$ and Re $\varepsilon_{x,y} > 0$, the equifrequency surface (EFS) is hyperbolic instead of elliptic as shown in Fig. 3(a). For this medium, it is more meaningful to discuss the energy flow. The group velocity refraction is governed by[13]

$$\tan\theta = -\sigma \tan\phi. \tag{5}$$

Here ϕ is the angle for the incident group velocity and θ is that for the refracted group velocity [see Fig. 3(b)]. The material property σ is defined and evaluated as[13]

$$\sigma \equiv -\frac{dk_z}{dk_{0z}} = -\frac{\sqrt{\varepsilon_x}}{\varepsilon_z}\frac{\sqrt{k_0^2 - k_x^2}}{\sqrt{k_0^2 - k_x^2/\varepsilon_z}}. \tag{6}$$

Here $k_{0z} = \sqrt{k_0^2 - k_x^2}$. One has $\sigma > 0$ for all propagating waves, thus, AANR[6] can be realized in this medium. The effective refractive index n_{eff} is related to σ through $n_{\text{eff}} \sin\theta = \sin\phi$. One has $n_{\text{eff}} \sim -\sigma^{-1}$. For small k_x the EFS can be approximated elliptically by $k_z \simeq \kappa - \sigma_0 k_{0z}$ with $\sigma_0 = -\sqrt{\varepsilon_x}/\varepsilon_z > 0$ and $\kappa = \sqrt{\varepsilon_x} k_0 (1 - 1/\varepsilon_z)$.

When σ is constant, then the phase across the lens $\Phi_z = k_{0z}(u+v) + k_z d = \kappa d$ is stationary and an image will be formed without aberration. Here u, v, and d obey the equation $u + v = \sigma d$ [Fig. 3(b)]. This is the lens equation for a generalized superlens. In this case, the refractive index n_{eff} is angle dependent, and one can achieve "perfect focusing" without an optical axis, as discussed in Ref. 13. Note that the Veselago lens has $\sigma = 1$, where the EFS is circular.

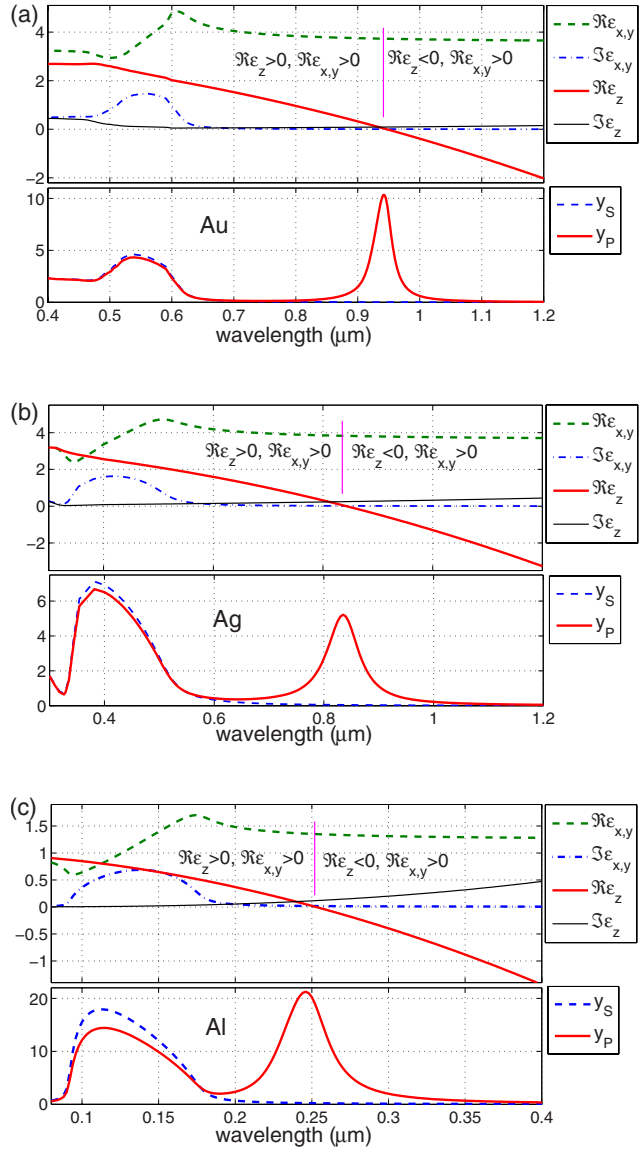

FIG. 2. (Color online) Effective permittivity and absorption spectra of metamaterials made of metallic nanowires embedded in dielectric masks for S- and P-polarized waves with incident angle 25°. The thickness of the metamaterials are all 500 nm. (a) 8% Au nanowires in alumina template, (b) 8% Ag nanowires in alumina template, (c) 10% Al nanowires in air. The dielectric constants ε_m are taken from Ref. 20. For simplicity we use $\varepsilon_a = 3$ for alumina in the infrared and the visible range. Dashed lines are for the S polarization and solid lines for the P polarization.

In the present anisotropic metamaterial, σ is angle dependent and not a constant because the EFS is hyperbolic and not elliptic;[13] hence, the lens has caustics, and the image is not "perfect." Nevertheless, a high quality image can be formed by the lens with $u + v = \sigma_{\text{eff}} d$ and $\sigma_{\text{eff}} < \sigma_0$. Furthermore, though the nonlocal effect[22–26] on effective permittivity indicates the limitation of Bruggeman's EMT, it will render the EFS to be more elliptic than hyperbolic; thus, it can reduce the caustics.

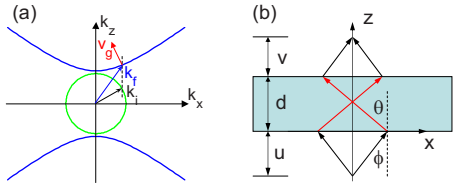

FIG. 3. (Color online) (a) Illustration of negative refraction and (b) superlens imaging of P-polarized waves by a slab of indefinite medium with Re $\varepsilon_z<0$ and Re $\varepsilon_x>0$. The blue/dark gray line is the EFS in this medium, and the green/light gray line is the corresponding EFS in the air. An incident plane wave with $\vec{k}_i$ will be refracted as $\vec{k}_f$, which has negative group refraction (red/gray arrow). The superlens has a lens equation $u+v=\sigma d$.

The composite medium with cylinder inclusion can be used for NR and superlens imaging in three-dimensional free space for frequencies below the surface plasmon frequency. These metamaterials do not support surface waves. The enhancement of subwavelength imaging resolution is still possible.[27–29] If the lens is curved, one may be able to use it as a magnifying hyperlens.[30,31] The currently studied multilayered structures[30–36] for NR, superlens, and hyperlens are two-dimensional reductions of these structures. The filling ratio $f=1/2$ is special for multilayered metal-dielectric structures. At this filling ratio, Re ε_x and Re ε_z will always have the opposite signs. This has been utilized to realize magnifying hyperlens.[30–32] Naturally available anisotropic dielectric crystals may be used to achieve NR[37] but cannot be used for superlens imaging.

Anisotropic metamaterials with embedded Au, Ag, Al nanowires can be used for superlens imaging in the infrared, visible, and ultraviolet, respectively. For example, for Al at $\lambda=326.3$ nm, $\varepsilon_m=-15.468+2.575i$,[20] a 10% filling ratio of Al nanowires in air gives $\varepsilon_x=1.301+0.010i$ and $\varepsilon_z=-0.647+0.258i$. A lens made of a flat slab of such medium has $\sigma_0=1.52$ and can have a maximum thickness 11.9 μm. The imaging effect of a point source by such a superlens is shown in Fig. 4(a). The angle-dependent lens property σ as shown in Fig. 4(b) leads to the presence of caustics, which can be reduced if multiple lenses are used.

For the propagating waves within the xy plane, NR and superlens imaging can be realized in a finite slab of such an anisotropic medium. In this case, for the P-polarized waves, one has $k_x=\sqrt{\varepsilon_z}\sqrt{k_0^2-k_z^2/\varepsilon_x}$. For $\lambda>\lambda_l$, Re $\varepsilon_z<0$, a free-suspending slab will support guided waves in the xy plane if $\sqrt{\text{Re }\varepsilon_x}>1$ and $k_z>\sqrt{\text{Re }\varepsilon_x}k_0$. These guided waves are backward waves with Re $k_x<0$. In this geometry, surface waves can be formed, which can lead to subwavelength imaging resolution. We point out that there is no need to sandwich this medium by perfect conductor waveguide plates as considered in Ref. 38.

For the S polarization, the medium with cylinder inclusion is isotropic with positive effective permittivity. The dispersion is given by $k_z^2=\varepsilon_y k_0^2-k_x^2$. No NR can be realized for this polarization.

There are two strategies to realize Re $\varepsilon_z<0$ and Re $\varepsilon_x>0$, depending on the wavelength $\lambda>\lambda_{sp}$ or $\lambda<\lambda_{sp}$. Sphere

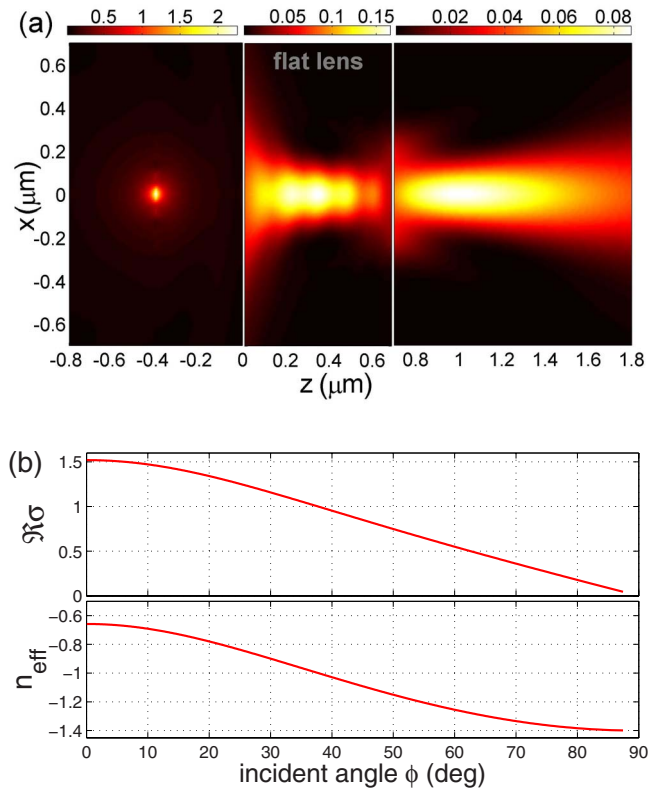

FIG. 4. (Color online) (a) Imaging by a superlens with $\varepsilon_x=1.301+0.010i$, $\varepsilon_z=-0.647+0.258i$, and thickness $d=0.7$ μm, at $\lambda=326.3$ nm. The point source is at $u=0.40$ μm and a focus is obtained at $v=0.30$ μm. The lens has $\sigma_{\text{eff}}=1.00$. Plotted is the intensity of the magnetic field, which is in the y direction. Evanescent waves of the source are included up to $k_x/k_0=3$. (b) Lens property σ and n_{eff} as functions of the incident angle.

inclusion will lead to isotropic permittivity. Only the cylinder or slab inclusion will lead us to the desired anisotropy. For $\lambda>\lambda_{sp}$, the cylinder axis should be along the z axis, which we have discussed in this Brief Report. The slab inclusion must be realized as a metallic grating as in Ref. 33. In this case, one has Re $\varepsilon_{y,z}<0$ and Re $\varepsilon_x>0$. Though loss is low in ε_x, NR is limited to the xz plane. We point out that the EMT theory gives a very simple explanation for the broadband AANR in the metallic grating.[33] Furthermore, the EMT is more accurate than the coupled-wave theory used in Ref. 33. We also point out that our numerical simulations indicate that AANR does not require the metallic grating to be periodic.

For $\lambda_p<\lambda<\lambda_{sp}$, indefinite medium can be realized if the cylinder axis is in the xy plane for the cylinder inclusion. If the cylinder axis is along the x axis, one has $\varepsilon_x=\varepsilon_{\text{eff}}(\infty)$ and $\varepsilon_{y,z}=\varepsilon_{\text{eff}}(1)$. For these wavelengths $-\varepsilon_a<\text{Re }\varepsilon_m<0$, one should have $1/2<f<\varepsilon_a/(\varepsilon_a-\text{Re }\varepsilon_m)$, high loss will be expected for ε_x. However, the slab inclusion, which is exemplified by the multilayered metal-dielectric structures considered in Refs. 34–36, will have Re $\varepsilon_z<0$ and Re $\varepsilon_{x,y}>0$ for $-\varepsilon_m/(\varepsilon_a-\text{Re }\varepsilon_m)<f<\varepsilon_a/(\varepsilon_a-\text{Re }\varepsilon_m)$ with low loss. For these structures,[34–36] Bruggeman's EMT may not be very precise to calculate the effective permittivity, but our imaging theory predicts that they are able to focus.

In summary, we have established an imaging theory of superlens made of nanoporous dielectric templates embedded with metallic nanowires with strong optical anisotropy. The effective permittivity of these media is obtained by Bruggeman's EMT. Our theory is successfully used to give simple explanation of recent predictions of NR and superlens focusing in multilayered[33–36] and 2D structures.[27,28] For frequencies lower than the longitudinal SPR frequency, these media are indefinite media.[21] The existence of Re $\varepsilon_z < 0$ and Re $\varepsilon_{x,y} > 0$ is manifested by the fact that there is a band cutoff for the TM modes and no band cutoff for the TE modes of 2D metal-dielectric photonic crystals. The homogenization,[17,39] including the nonlocal effect[22–26] of 2D photonic crystals, provides direct and more accurate ways to calculate the effective indices beyond EMT. Unlike resonant metamaterials, which are sensitive to disorder,[40] these nanowire media has large tolerance on disorder. These extremely anisotropic metamaterials are broadband and can be used for NR, superlens, and hyperlens applications in 3D for frequencies from infrared up to ultraviolet.

We thank L. Menon, B. D. F. Casse, and R. Banyal for useful discussions. This work was supported by the Air Force Research Laboratories, Hanscom through FA8718-06-C-0045 and the National Science Foundation through PHY-0457002.

*Electronic address: w.lu@neu.edu

[1] V. G. Veselago, Sov. Phys. Usp. **10**, 509 (1968).
[2] R. A. Shelby, D. R. Smith, and S. Shultz, Science **292**, 77 (2001).
[3] V. M. Shalaev, Nat. Photonics **1**, 41 (2007).
[4] J. B. Pendry, Phys. Rev. Lett. **85**, 3966 (2000).
[5] M. Notomi, Phys. Rev. B **62**, 10696 (2000).
[6] C. Luo, S. G. Johnson, J. D. Joannopoulos, and J. B. Pendry, Phys. Rev. B **65**, 201104(R) (2002).
[7] P. V. Parimi, W. T. Lu, P. Vodo, J. Sokoloff, J. S. Derov, and S. Sridhar, Phys. Rev. Lett. **92**, 127401 (2004); P. V. Parimi, W. T. Lu, P. Vodo, and S. Sridhar, Nature (London) **426**, 404 (2003).
[8] O. Jessensky, F. Müller, and U. Gösele, Appl. Phys. Lett. **72**, 1173 (1998).
[9] W. Lee, R. Ji, U. Gösele, and K. Nielsch, Nat. Mater. **5**, 741 (2006).
[10] M. S. Sander and L.-S. Tan, Adv. Funct. Mater. **13**, 393 (2003); O. Rabin, P. R. Herz, Y.-M. Lin, A. I. Akinwande, S. B. Cronin, and M. S. Dresselhaus, *ibid.* **13**, 631 (2003).
[11] B. G. McMillan, L. E. A. Berlouis, F. R. Cruickshank, D. Pugh, and P.-F. Brevet, Appl. Phys. Lett. **86**, 211912 (2005).
[12] L. Menon, W. T. Lu, A. L. Friedman, S. Bennett, D. Heiman, and S. Sridhar, Appl. Phys. Lett. (to be published).
[13] W. T. Lu and S. Sridhar, Opt. Express **13**, 10673 (2005).
[14] D. E. Aspnes, Am. J. Phys. **50**, 704 (1982).
[15] A. Sihvola, *Electromagnetic Mixing Formulas and Applications* (Institute of Electrical Engineers, London, 1999).
[16] T. G. Mackay and A. Lakhtakia, Opt. Commun. **234**, 35 (2004).
[17] The homogenization of 2D photonic crystals gives $D \sim 1$ and $D \gg 1$ for $\varepsilon_{x,y}$ and ε_z, respectively. There is not much difference in our subsequent discussions if more accurate expression is used. For homogenization of photonic crystals, see P. Halevi, A. A. Krokhin, and J. Arriaga, Phys. Rev. Lett. **82**, 719 (1999); P. Halevi, A. A. Krokhin, and J. Arriaga, *ibid.* **86**, 3211 (2001); A. A. Krokhin and E. Reyes, *ibid.* **93**, 023904 (2004).
[18] Y.-Y. Yu, S. Chang, C. Lee, and C. R. Wang, J. Phys. Chem. B **101**, 6661 (1997).
[19] R. Atkinson, W. R. Hendren, G. A. Wurtz, W. Dickson, A. V. Zayats, P. Evans, and R. J. Pollard, Phys. Rev. B **73**, 235402 (2006).
[20] *Optical Properties of Metals*, edited by J. H. Weaver (Fachinformationszentrum, Karlsruhe, Germany, 1981).
[21] D. R. Smith and D. Schurig, Phys. Rev. Lett. **90**, 077405 (2003); D. R. Smith, P. Kolinko, and D. Schurig, J. Opt. Soc. Am. B **21**, 1032 (2004).
[22] A. L. Pokrovsky and A. L. Efros, Phys. Rev. B **65**, 045110 (2002).
[23] P. A. Belov, R. Marques, S. I. Maslovski, I. S. Nefedov, M. Silveirinha, C. R. Simovski, and S. A. Tretyakov, Phys. Rev. B **67**, 113103 (2003); P. A. Belov and C. R. Simovski, Phys. Rev. E **72**, 026615 (2005).
[24] M. G. Silveirinha, Phys. Rev. E **73**, 046612 (2006).
[25] C. R. Simovski and S. A. Tretyakov, Phys. Rev. B **75**, 195111 (2007).
[26] J. Elser, V. A. Podolskiy, I. Salakhutdinov, and I. Avrutsky, Appl. Phys. Lett. **90**, 191109 (2007).
[27] A. Ono, J. I. Kato, and S. Kawata, Phys. Rev. Lett. **95**, 267407 (2005).
[28] M. G. Silveirinha, P. A. Belov, and C. R. Simovski, Phys. Rev. B **75**, 035108 (2007).
[29] G. Shvets, S. Trendafilov, J. B. Pendry, and A. Sarychev, Phys. Rev. Lett. **99**, 053903 (2007).
[30] Z. Jacob, L. V. Alekseyev, and E. Narimanov, Opt. Express **14**, 8247 (2006).
[31] A. Salandrino and N. Engheta, Phys. Rev. B **74**, 075103 (2006).
[32] Z. Liu, H. Lee, Y. Xiong, C. Sun, and X. Zhang, Science **315**, 1686 (2007); I. I. Smolyaninov, Y.-J. Hung, and C. C. Davis, *ibid.* **315**, 1699 (2007).
[33] X. Fan, G. P. Wang, J. C. W. Lee, and C. T. Chan, Phys. Rev. Lett. **97**, 073901 (2006).
[34] H. Shin and S. Fan, Appl. Phys. Lett. **89**, 151102 (2006).
[35] B. Wood, J. B. Pendry, and D. P. Tsai, Phys. Rev. B **74**, 115116 (2006).
[36] A. J. Hoffman, L. Alekseyev, S. S. Howard, K. J. Franz, D. Wasserman, V. A. Podolskiy, E. E. Narimanov, D. L. Sivco, and C. Gmachl, Nat. Mater. **6**, 946 (2007).
[37] Y. Zhang, B. Fluegel, and A. Mascarenhas, Phys. Rev. Lett. **91**, 157404 (2003).
[38] V. A. Podolskiy and E. E. Narimanov, Phys. Rev. B **71**, 201101(R) (2005).
[39] X. Hu, C. T. Chan, J. Zi, M. Li, and K.-M. Ho, Phys. Rev. Lett. **96**, 223901 (2006).
[40] M. V. Gorkunov, S. A. Gredeskul, I. V. Shadrivov, and Y. S. Kivshar, Phys. Rev. E **73**, 056605 (2006).